*Environ. Sci. Technol.* **2002**, *36,* 1712−1719

# Scavenging of As from Acid Mine Drainage by Schwertmannite and Ferrihydrite: A Comparison with Synthetic Analogues

L. CARLSON,[†] J. M. BIGHAM,*[,‡] U. SCHWERTMANN,[§] A. KYEK,[∥] AND F. WAGNER[∥]

*University of Helsinki, FIN-00171 Helsinki, Finland, School of Natural Resources, The Ohio State University, Columbus, Ohio 43210, Lehrstuhl für Bodenkunde, Technische Universität München, D-85350 Freising-Weihenstephan, Germany, and Physik-Department E 15, Technische Universität München, D-85747 Garching, Germany*

Ochreous precipitates containing 5.5−69.8 g/kg As were isolated from mine drainage in Finland and were composed of schwertmannite, ferrihydrite, and goethite. Schwertmannite formation was favored at pH 3−4, but its structure was degraded at high As levels. A series of coprecipitates were therefore prepared from mixed iron arsenate/sulfate solutions to define the limits of schwertmannite stability. Schwertmannite was replaced as the dominant phase by a poorly crystalline iron$^{III}$ hydroxy arsenate (FeOHAs) when As/Fe mole ratios exceeded 0.15. The FeOHAs gave an X-ray diffraction pattern similar to that obtained from an "amorphous" iron$^{III}$ arsenate (As/Fe = 1.0) with broad peaks at 0.30 and 0.16 nm. The FeOHAs possessed a magnetic hyperfine field of 41.9 T at 4.2 K that was intermediate to those of schwertmannite (46.1 T) and the iron$^{III}$ arsenate (24.8 T). These data indicate a strong disruptive effect of arsenate on magnetic ordering and structure development in schwertmannite. Equilibration of 0.01 M arsenate solutions with freshly prepared schwertmannite and 2-line ferrihydrite at pH 3.0 for up to 60 d gave sorbed As contents of 175 and 210 g/kg, respectively. Arsenate sorption degraded the host schwertmannite and ferrihydrite, perhaps due to the formation of an FeOHAs surface phase.

## Introduction

Arsenic exposure is a major human health concern (*1*). Even though As is normally present at concentrations lower than 50 $\mu$g/L in natural waters (*2*), locally elevated levels may be produced by dissolution of sulfide minerals such as arsenopyrite (FeAsS), cobaltite (CoAsS), or arsenical pyrite ($FeS_2$) (*3*, *4*). Such minerals are present in many economic ore deposits and may be introduced to the weathering zone in leach piles and mine spoils (e.g., refs *5* and *6*). Acid leach waters created by natural weathering or by hydrometallurgical processing are usually also enriched with both sulfate and Fe. The oxidation and hydrolysis of Fe produces secondary precipitates that directly influence the activity of As in associated solutions.

Because sorption is thought to be an important mechanism controlling As concentrations in most aquatic systems, the retention of As by iron$^{III}$ oxide surfaces has been widely studied with pH, background electrolyte concentration, and oxidation state (i.e., arsenate vs arsenite) as major experimental variables (e.g., ref *7*). Laboratory sorption studies on pre-prepared mineral sorbents are important to an understanding of bonding mechanisms, but they do not guarantee that the sorbent is relevant to natural systems. Nor do they reflect the fact that mineral precipitation from acid sulfate waters involves the spontaneous formation of solid phases from mixed Fe, S, and As systems where coprecipitation is likely to occur. Coprecipitation in this context means that As may precipitate as a stoichiometric compound such as scorodite ($FeAsO_4 \cdot 2H_2O$), as a poorly ordered phase of variable composition such as pitticite ($Fe^{III}-SO_4-As_2O_5-H_2O$) (*8*), or as a solid−solution impurity in some other mineral species. For example, an Fe-rich precipitate resembling 2-line ferrihydrite ($Fe_5HO_8 \cdot 4H_2O$) but containing 50−60 g/kg As has recently been identified as a product from the mixing of hydrothermal fluids and seawater along the coast of Ambitle Island, Papua New Guinea (*9, 10*).

Coprecipitation phenomena involving As and Fe have also been widely studied by hydrometallurgists as a means of removing As from process wastewaters. The solubilities of both crystalline scorodite and "amorphous" iron$^{III}$ arsenate ($FeAsO_4 \cdot xH_2O$) have been considered in a number of experiments designed to evaluate the suitability of such compounds for As stabilization (*11*−*13*). A general conclusion of these studies is that scorodite and amorphous iron$^{III}$ arsenate are unstable at pH >2 and at As concentrations <0.01 *m*. These and other authors (e.g., ref *14*) have also noted that As-rich precipitates of increased stability are formed when the As/Fe mole ratio is <0.5. Krause and Ettel (*15*) refer to such X-ray amorphous compounds as basic iron$^{III}$ arsenates [$FeAsO_4 \cdot xFe(OH)_3$]; however, Robins et al. (*16*) consider this concept to be inappropriate and favor adsorption of arsenate on "iron$^{III}$ hydroxide" as the method of As retention when Fe and As are coprecipitated from solutions with As/Fe < 1.0. Spectroscopic studies by Waychunas et al. (*17*) also appear to indicate that arsenate behaves as an adsorbate on ferrihydrite when Fe and As are coprecipitated at pH 8.0.

A major problem in clarifying the coprecipitation/sorption issue in compounds with As/Fe <1 is that the mineralogical identity of relevant natural specimens has generally been left undefined. Studies by Bigham et al. (*18*, *19*) have shown that a poorly crystalline oxyhydroxysulfate of iron with a formula ranging between $Fe_8O_8(OH)_6SO_4$ and $Fe_8O_8(OH)_{4.5}(SO_4)_{1.75}$ is often the primary component of precipitates formed from sulfate-rich mine waters at pH 2.5−4.5. This phase, now recognized as the mineral schwertmannite (*20*), is believed to have a structure similar to that of akaganéite ($\beta$-FeOOH) with sulfate serving as a stabilizing surface and/or structural component. Among the mine drainage precipitates collected to date are some rich in As and deficient in S, raising the question of whether schwertmannite, ferrihydrite, or some other mineral phase is the primary host for As. Consequently, the objectives of the current study were to (i) characterize a series of natural, As-bearing precipitates from acid mine effluents and (ii) compare the properties of the natural samples to those of synthetic specimens prepared by coprecipitation from iron$^{III}$−arsenate−sulfate solutions

* Corresponding author telephone: (614)292-9066; fax: (614)292-7432; e-mail: bigham.1@osu.edu.
[†] University of Helsinki.
[‡] The Ohio State University.
[§] Technische Universität München, Freising-Weihenstephan.
[∥] Technische Universität München, Garching.


10.1021/es0110271 CCC: $22.00 
Published on Web 03/07/2002

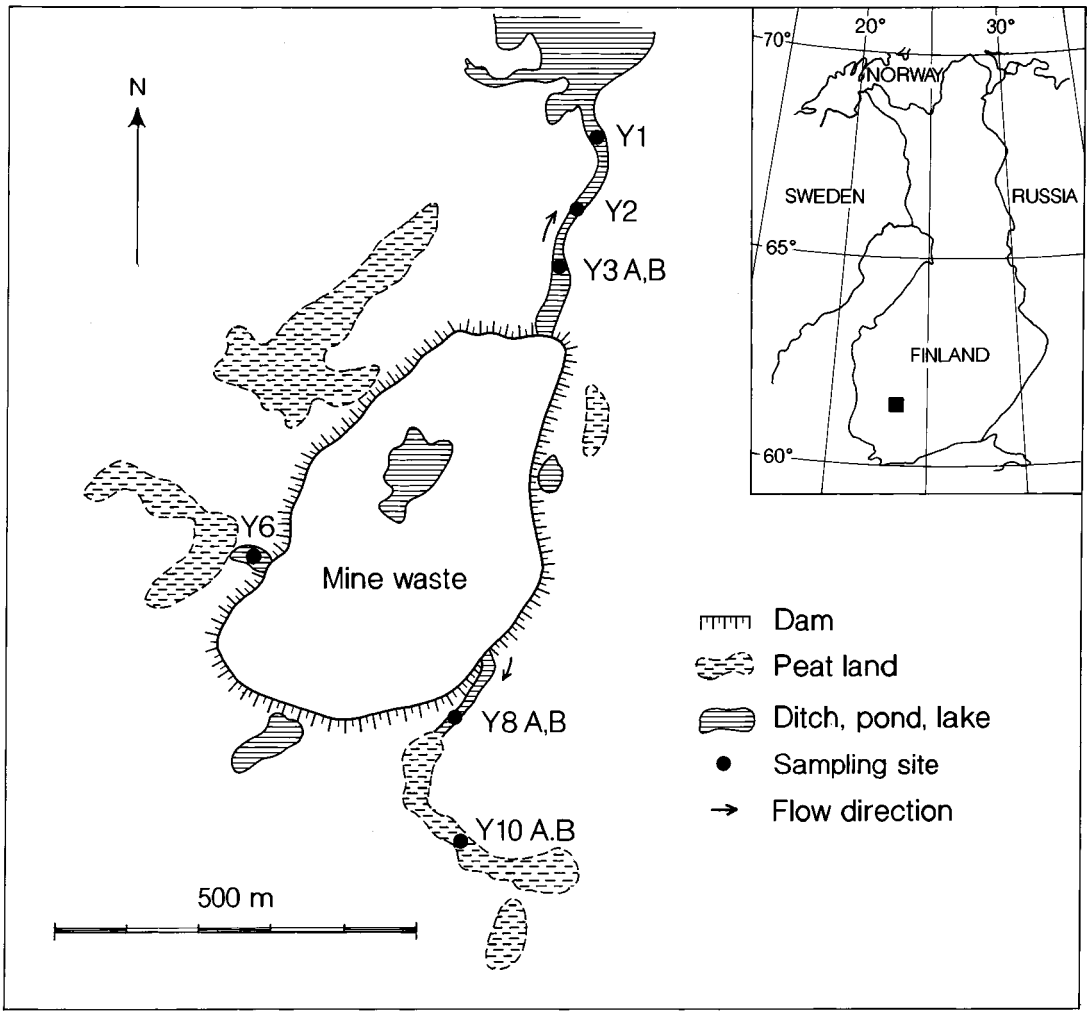


**FIGURE 1. Location and distribution of sampling sites around the tailings and waste area of the Paroistenjärvi sulfide mine at Ylöjärvi, Finland.**

and by sorption of arsenate on pre-prepared schwertmannite and ferrihydrite at pH 3.0.

## Materials and Methods

**Natural Samples.** The Paroistenjärvi Mine at Ylöjärvi, Finland (61°36′ N, 23°30′ E), was closed in 1966. The local sulfide deposit (pyrite, chalcopyrite, arsenopyrite, pyrrhotite) was extracted mainly for Cu but had an average As content of 6 g/kg. Spoil containing both waste rock and tailings sand was covered with a layer of sediment and vegetated following closure of the mine. Today, water draining the spoil gathers in small ponds and flows through ditches to rivers and lakes. The bottoms of the ponds and ditches are covered with ochreous precipitates. Both water and precipitates were collected at several locations around the spoil to assess the degree of environmental contamination (Figure 1). The specimens were kept cool and dark during transport to the laboratory where the precipitates were subsequently concentrated by repeated gravity sedimentation in deionized water. Organic matter and detrital mineral grains with effective spherical diameter >2 $\mu$m were removed according to Stokes' law calculations. Following enrichment of the <2-$\mu$m fraction, the solids were dried at 60° C. No detectable mineralogical differences were observed by drying at 60° C as compared to freeze-drying.

**Synthetic Coprecipitates.** A series of synthetic specimens was prepared by forced hydrolysis of 0.02 M iron$^{III}$ nitrate solutions using a synthesis protocol similar to that proposed for schwertmannite (*18*) except that graded amounts of $SO_4$ and $AsO_4$ were employed. Specifically, background solutions (1000 mL total volume) were prepared by mixing 0.013 M $Na_2HAsO_4 \cdot 7H_2O$ and 0.02 M $Na_2SO_4$ in volume ratios ($AsO_4$/$SO_4$) of 0/1000, 31/969, 62/938, 125/875, 250/750, 500/500, 750/250, and 1000/0 to yield As/(As+S) mole ratios ranging between 0 and 1. The mixed $AsO_4/SO_4$ solutions were then preheated to 60 °C, and Fe was added as powdered $Fe(NO_3)_3 \cdot 9H_2O$ (8.32 g/L) giving initial As/Fe mole ratios ranging from 0 (0/1000) to 0.65 (1000/0). Following hydrolysis for 12 min at 60 °C, the resulting suspensions (pH values ranged from 1.7 to 2.2) were cooled to room temperature (RT), transferred to cellulose dialysis bags with an average pore radius of 2.4 nm, and dialyzed against deionized water for 30 d. The precipitates were then freeze-dried and stored.

For comparative purposes, an "amorphous" iron$^{III}$ arsenate with As/Fe = 1 was prepared following the general method of Krause and Ettel (*13*). Briefly, 121.2 g of solid $Fe(NO_3)_3 \cdot 9H_2O$ was added to 1 L of a 0.3 M $NaH_2AsO_4$ solution that had been preheated to 80 °C. The resulting suspension was maintained at this temperature for 24 h with occasional shaking. The suspension was then cooled, dialyzed against deionized water for 14 d, frozen, and freeze-dried.

**Sorption Samples.** Synthetic schwertmannite (identical to the coprecipitate with As/Fe = 0) was prepared as described in the previous section without drying the solid from aqueous suspension. Aliquots of suspension containing the equivalent of 0.01 M Fe were then transferred to 250-mL centrifuge

bottles and diluted to 200 mL. The equivalent of 0.01 M As (as $NaH_2AsO_4 \cdot 7H_2O$) was added while stirring, and the pH was immediately adjusted to 3.0 with 0.5 M HCl. Subsamples were equilibrated at room temperature for 1, 10, 20, 30, and 60 d after which they were washed by centrifugation, frozen, and freeze-dried. All subsamples were then subjected to chemical and X-ray diffraction (XRD) analysis.

Samples of 2-line ferrihydrite were synthesized by adding 4.04 g of $Fe(NO_3)_3 \cdot 9H_2O$ (0.01 M Fe) to 50 mL of deionized water. Approximately 15.5 mL of 2 M NaOH was then added to each sample while vigorously stirring the suspension. The final increments of NaOH were added dropwise to bring the pH between 7.0 and 8.0. The precipitates were centrifuge-washed four times and then dispersed in 200 mL of deionized water. The equivalent of 0.01 M As (as $NaH_2AsO_4 \cdot 7H_2O$) was added while stirring, and the pH was adjusted to 3.0 with 0.5 M HCl. Subsamples were equilibrated at room temperature for 1, 10, 20, 30, and 60 d after which time they were washed by centrifugation, frozen, and freeze-dried. All subsamples were then subjected to chemical and XRD analysis.

**Analytical Methods.** Water samples were analyzed in the field for pH. The determination of $Fe^{2+}$ was accomplished by mixing 10 mL of sample in the field with 0.5 mL of a solution containing 272 g/L sodium acetate and 0.25 mL of a 0.3% solution of 2,2-dipyridyl in water. The samples were kept cool and dark during transport to the laboratory where the absorbance was immediately read at 522 nm. Total Fe ($Fe_t$) was measured in the same manner after reducing $Fe^{3+}$ with 0.25 mL of a 10% hydroxylamine hydrochloride solution. Sulfate and Cl were measured by ion chromatography. Arsenic was determined following reduction of all dissolved As to the trivalent state with KI and $SnCl_2$. The reduced As was then liberated in the presence of elemental Zn and absorbed in a solution of silver diethyldithiocarbamate in chloroform−quinoline. The reddish-brown As complex was quantified colorimetrically at 545 nm (*21*). Mn, Cu, and Zn were determined by atomic absorption spectroscopy.

Fe, As, and S in the natural and synthetic precipitates were determined by using ICP-AES (Jobin Yvon 70 Plus instrument) after dissolution of the oxide fractions in pH 3.0 ammonium oxalate (*22*). X-ray diffraction analyses were obtained from backfill powder mounts using either CoKα or CuKα radiation and a Philips goniometer equipped with a diffracted beam monochromator and a 1° divergence slit. The specimens were scanned from 10 to 80° 2$\theta$ in increments of 0.05° with 20 s counting time. The digitized scans were then modeled with the FIT curve program of Janik and Raupach (*23*) as modified by H. Stanjek (unpublished data).

Infrared (FTIR) absorption spectra were obtained from 5 mg of powdered sample mixed with 195 mg of KBr. The spectra were recorded with a Mattson-Polaris FTIR equipped with a Harrick "Preying Mantis" cell. Diffuse reflectance (DRIFT) spectra were collected as the average of 100 sample scans at 1 $cm^{-1}$ resolution. The spectra were analyzed using the computer program, Lab Calc, obtained from Galactic Industries. Surface area measurements were made by the single-point BET method (ASTM D4567) using a Micromeritics FlowSorb II 2300 instrument and $N_2$ as the adsorbate. Transmission electron microscopy (TEM) was conducted with a Philips 300A or a JEOL 100CX electron microscope operated at 60 kV. The colors of the synthetic precipitates were determined with a Minolta CR-200 Chroma Meter with 3−6 replications of each measurement.

Mössbauer spectra were recorded at room temperature and at 4.2 K (with temperature scans between 20 and 70 K in some cases) using a velocity drive equipped with a $^{57}Co$−Rh source in sinusoidal mode. Isomer shifts were derived with respect to this source, and a metallic iron foil was used for calibration purposes. The spectra were fitted with sets of split Gaussian distributions of Lorentzian-shaped lines for the magnetic sextets and quadrupole doublets (*24*). Hyperfine fields, $B_{hf}$, were calculated as average values.

**TABLE 1. Chemistry of Paroistenjärvi Water Samples[a]**

| site | pH | $Fe^{2+}$ | $Fe_t$ | As | $SO_4$ | Cl | Mn | Cu | Zn |
|---|---|---|---|---|---|---|---|---|---|
| Y1 | 4.8 | 2.4 | 2.5 | 0.15 | 168 | <1 | 0.3 | 0.5 | 0.1 |
| Y2 | 5.1 | 18.8 | 19.0 | 0.37 | 376 | <1 | 2.3 | 2.6 | 0.5 |
| Y3A | 5.8 | 66.1 | 74.1 | 0.39 | 503 | <1 | 5.7 | 11.9 | 2.2 |
| Y3B | 3.1 | nd[b] | 78.0 | 0.39 | 872 | 6.7 | 7.6 | 19.8 | 3.2 |
| Y6 | 3.4 | nd | 0.5 | 0.14 | 653 | <1 | 3.9 | 3.2 | 2.2 |
| Y8 | 3.1 | 13.9 | 38.0 | 0.14 | 705 | 4.4 | 3.6 | 3.6 | 1.9 |
| Y10 | 5.7 | 0.4 | 0.6 | 0.01 | 222 | <1 | 1.4 | 0.7 | 0.4 |

[a] All units (expect for pH) in mg/L. [b] nd, not determined.

## Results and Discussion

**Field Water Chemistry.** Water that flows directly to the surface from the Paroistenjärvi spoil heap (sites Y3B, Y6, and Y8) (Figure 1) has a low pH (~3) and is enriched in dissolved Fe, $SO_4$, and As as well as Mn, Cu, and Zn (Table 1). Chloride is low as compared to $SO_4$. Where drainage remains exposed to the atmosphere in local ditches and ponds, the oxidation and precipitation of Fe and the coprecipitation/sorption of other elements causes the concentrations of Fe, $SO_4$, As, etc. to decline. Note, for example, the downstream trends associated with samples Y3B → Y1 and Y8 → Y10 (Figure 1, Table 1). The pH increases (4.0−6.0) downstream, especially where drainage comes in contact with vegetation or peat, as at site Y10.

**Properties of the Natural Precipitates.** The mineralogy and chemistry of ochreous precipitates from the drainage waters are closely linked to the geochemical conditions at each sampling site (Table 2). Those precipitates formed at pH 3−4 in the presence of adequate sulfate are composed primarily of schwertmannite (samples Y3B, Y6, and Y8A&B). Those influenced by higher pH waters contain significant admixtures of ferrihydrite and/or goethite.

Schwertmannite yields an 8-peak XRD pattern, has an S/Fe mole ratio ranging between 0.125 and 0.21, and typically forms fibrous aggregates that are 200−500 nm in diameter. Sample Y3B (Figures 2 and 3a, Table 2) is a good example. Most of the Paroistenjärvi samples have S/Fe ratios near the lower end (Table 2) of the normal range for schwertmannite due to relatively low initial concentrations of sulfate in solution and to the aforementioned admixtures of ferrihydrite (e.g., samples Y10A&B) or goethite. In addition, dissolved arsenate in the mine effluent apparently competes with sulfate for sorption/coprecipitation sites. Sample Y6, for example, appears to be a relatively pure schwertmannite but is notable for its low S and corresponding high As content (Table 2). Its XRD pattern is similar to those of schwertmannites containing more sulfate except there is a marked reduction in the intensity of the 0.5-nm peak and a high background to peak ratio below 50° 2$\theta$ (Figure 2). The infrared spectrum from this sample (Figure 4) also shows diminished intensities for characteristic sulfate bands at 1130, 1040, 970, and 610 $cm^{-1}$ but has a relatively strong band at 840 $cm^{-1}$ produced by the symmetric stretching vibration of As−OFe bonds (*25*, *26*).

Ferrihydrite is typically formed from mine drainage solutions that are rich in organics or that have pH values exceeding 5 (*19*). This pH−mineral relationship is consistent with the observed mineralogy of samples from sites Y2, Y3A, and Y10A&B that contain, besides schwertmannite, significant amounts of ferrihydrite as judged from high background intensities and broad, asymmetric XRD peaks at 0.25 and 0.15 nm (Figure 2). The Mössbauer spectra from samples Y10A&B show asymmetric sextets at 4.2 K (Figure 5a,b) with average weighted hyperfine fields of 45.7 and 46.7 T,

**TABLE 2. Chemical and Mineralogical Composition of Natural Precipitates**

| sample | Fe (g/kg) | As (g/kg) | S (g/kg) | Si (g/kg) | Mn (g/kg) | Cu (mg/kg) | Zn (mg/kg) | As/Fe (mol/mol) | S/Fe (mol/mol) | As/(As+S) (mol/mol) | mineralogy[a] |
|---|---|---|---|---|---|---|---|---|---|---|---|
| Y1 | 356 | 6.06 | 28.4 | 3.0 | 0.42 | 714 | 56 | 0.01 | 0.14 | 0.084 | Sh, Gt |
| Y2 | 339 | 9.96 | 22.4 | 7.8 | 0.20 | 2910 | 57 | 0.02 | 0.11 | 0.160 | Sh, Fh |
| Y3A | 289 | 8.25 | 27.0 | 11.5 | 0.15 | 3675 | 43 | 0.02 | 0.16 | 0.116 | Sh, Fh |
| Y3B | 456 | 15.3 | 36.0 | 1.9 | 0.12 | 345 | 20 | 0.03 | 0.14 | 0.154 | Sh |
| Y6 | 347 | 69.8 | 12.7 | 2.8 | 0.10 | 825 | 30 | 0.15 | 0.06 | 0.702 | Sh |
| Y8A | 399 | 5.45 | 32.4 | 1.9 | 0.29 | 1470 | 91 | 0.01 | 0.14 | 0.067 | Sh, Gt |
| Y8B | 384 | 9.44 | 27.7 | 2.8 | 0.46 | 1905 | 55 | 0.02 | 0.13 | 0.127 | Sh |
| Y10A | 244 | 6.05 | 10.3 | 25.5 | 0.34 | 2910 | 226 | 0.02 | 0.07 | 0.201 | Fh, Sh |
| Y10B | 350 | 22.3 | 4.3 | 25.8 | 0.50 | 3020 | 355 | 0.05 | 0.02 | 0.689 | Fh, Gt, Sh |

[a] Fh, ferrihydrite; Gt, goethite; Sh, schwertmannite. Listed according to relative abundance.

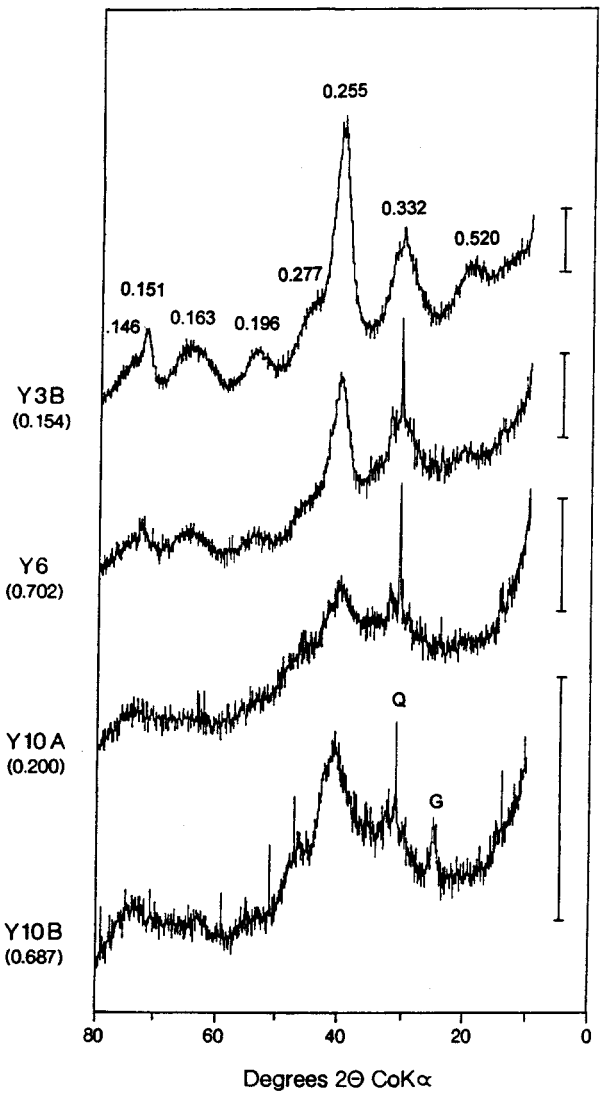


**FIGURE 2. Selected X-ray diffractograms from the mine drainage precipitates described in Table 1. Patterns identified by sample number and As/(As+S) mole ratios of the solids. Peak positions are in nm. G, goethite; Q, quartz. Scale bars correspond to 200 counts per second.**

respectively. Both values are intermediate to those typically reported for schwertmannite and ferrihydrite. Temperature scans between 20 and 70 K show that whereas magnetic order essentially disappears at 50 K for sample Y10A, it is still present at 60 K with sample Y10B. This variation reflects differences in crystal order or particle size that correspond with observed peak broadening in the XRD patterns and that may be influenced by coprecipitated As (see discussion under properties of synthetic coprecipitates).

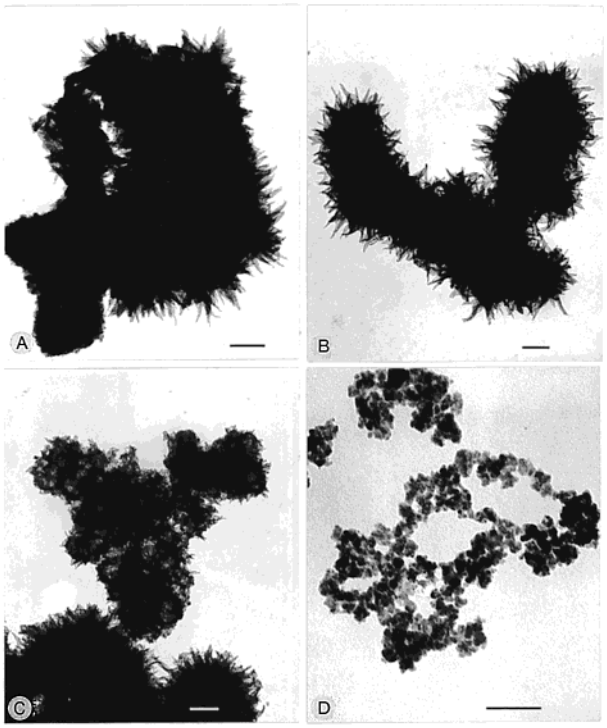


**FIGURE 3. TEM photographs taken from (a) natural sample Y3B, (b) synthetic coprecipitate with solid As/(As+S) = 0.233, (c) synthetic coprecipitate with solid As/(As+S) = 0.611, and (d) synthetic coprecipitate with solid As/(As+S) = 0.910. Bar = 100 nm.**

The Cu, Zn (in most cases), and Si contents of the Paroistenjärvi samples containing ferrihydrite are elevated as compared to other samples (Table 2) and probably reflect enhanced sorption of these species due to higher local pH conditions. Copper may also be complexed with organic matter (*27*). Natural ferrihydrites often contain up to 90 g/kg Si, and Rancourt et al. (*10*) recently reported an anticorrelation between Si and As suggesting competition for complexation sites on ferrihydrite surfaces. Competitive sorption between silicate and arsenate may thus account for lower As (and S) concentrations in most of the Paroistenjärvi samples containing ferrihydrite (Table 2). Sample Y10B, with 22.3 g/kg As, is a notable exception; however, the diagnostic IR band for $HAsO_4^{2-}$ at 840 $cm^{-1}$ is weak or absent in the precipitates from this site (Figure 4), suggesting that As may be present as a different mineral phase.

**Properties of Synthetic Coprecipitates.** The strong affinity of arsenate relative to sulfate for Fe is clear from a comparison of the As/(As+S) mole ratios of the synthetic coprecipitates with those of the initial solutions (Table 3). Arsenate is much

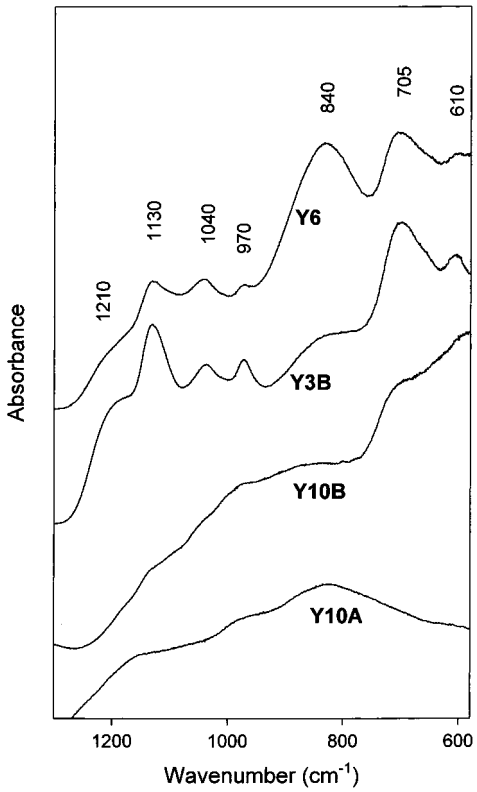


**FIGURE 4. DRIFT spectra from natural samples Y3, Y6, and Y10A&B.**

more strongly partitioned into the solid phase than is sulfate, especially at low initial solution ratios.

**X-ray Data.** The As-free sample in this series is a typical schwertmannite in terms of its chemistry (41 g/kg S; S/Fe = 0.15) and XRD profile (Table 3, Figure 6). As the As/(As+S) ratio increases, all XRD peaks for schwertmannite weaken and are gradually replaced by broad peaks at 0.31 and 0.16 nm (Figure 6). The 200,111 peak of schwertmannite at 0.51 nm is especially sensitive to the presence of As and disappears when the solid-phase concentration exceeds approximately 100 g/kg. This behavior is consistent with that noted previously for natural sample Y6 (Figure 2). The position of this peak and those at 0.33, 0.17, and 0.15 nm also appear to shift with increasing As content; however, these shifts are likely due to overlap with the two new, broad peaks that gradually form as more and more As is added (Figure 6).

We attribute these new peaks to a high As phase formed at the expense of schwertmannite. The XRD profile of this phase is similar in appearance to that of 2-line ferrihydrite, but the peak positions occur at significantly higher d values (0.31 and 0.16 nm vs 0.25 and 0.15 nm). The peak positions are, in fact, very similar to those of the pale yellow, amorphous iron$^{III}$ arsenate prepared from a solution with As/Fe = 1.0 by the method of Krause and Ettel (*13*) (Figure 7). The yellowish-brown colors (Munsell hue = 7.6−8.2 YR) of coprecipitates from the mixed arsenate/sulfate solutions (Table 3) presumably reflect a more oxidic character. We therefore refer to the high As phase as a poorly crystalline iron$^{III}$ hydroxyarsenate (FeOHAs) to distinguish it from the yellowish (Munsell hue = 1.6 Y) iron$^{III}$arsenate of Krause and Ettel (*13*). A quantification of schwertmannite and the FeOHAs phase using area ratios for the 0.255-nm peak of schwertmannite and the 0.31-nm peak of FeOHAs again demonstrates the strong preference of the solid phase for arsenate as compared to sulfate (Figure 8). The As contents of coprecipitates formed at solution As/(As+S) ratios <0.18 are lower than achieved by maximum sorption at pH 3.0 (see later discussion) and suggest that the FeOHAs phase may form prior to the saturation of sorption sites on the schwertmannite surface.

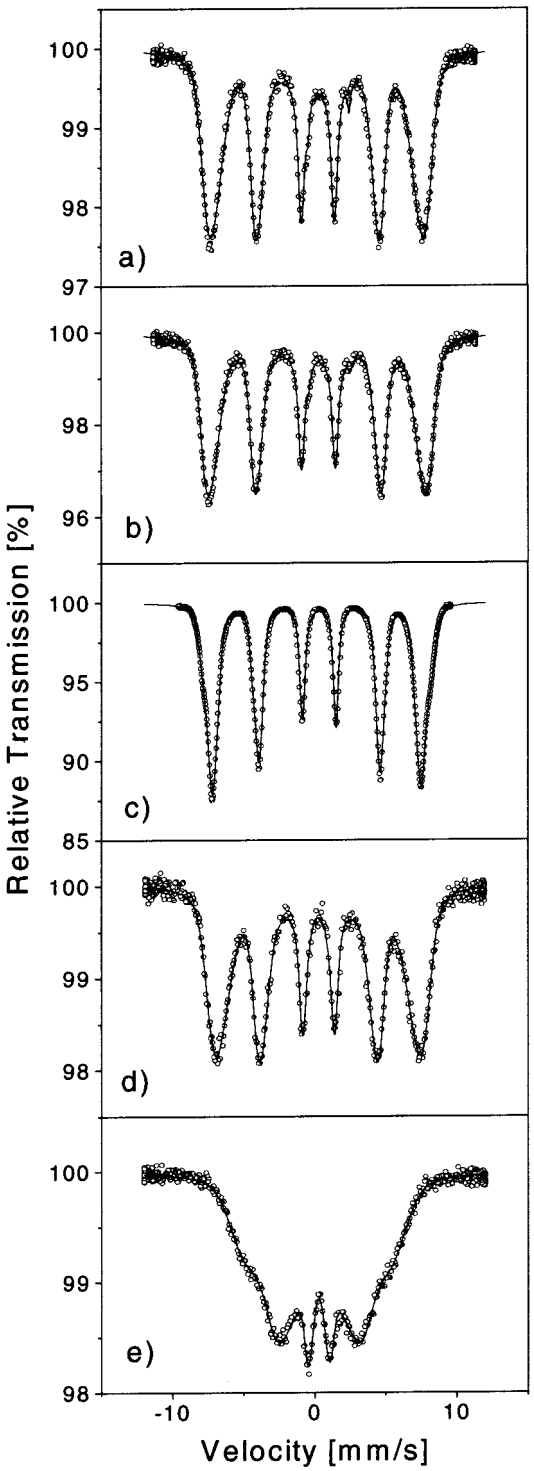


**FIGURE 5. Mössbauer spectra taken at 4.2 K from (a) natural sample Y10A, (b) natural sample Y10B, (c) synthetic schwertmannite, (d) synthetic FeOHAs with As/(As+S) = 1.0, and (e) synthetic iron$^{III}$ arsenate.**

**Morphology and Surface Area.** The As-free synthetic sample displays the pin cushion morphology (not shown) and high specific surface area (Table 3) that are typical of schwertmannite (*18*). At low As/(As+S) ratios (0.02−0.39) this morphology is retained, but the needles become blunted (Figure 3b) and the surface area decreases markedly. At intermediate As/(As+S) ratios, the rounded aggregates become thinner with porous centers indicating degradation of the schwertmannite particles (Figure 3c). Finally, as the As/(As+S) ratio rises above 0.8, the surface area increases to

**TABLE 3. Chemical and Physical Properties of Synthetic Coprecipitates and Sorption Samples**

| solution As/(As+S) (mol/mol) | Fe (g/kg) | As (g/kg) | S (g/kg) | As/Fe (mol/mol) | S/Fe (mol/mol) | As/(As+S) (mol/mol) | SSA[a] ($m^2$/g) | color[b] |
|---|---|---|---|---|---|---|---|---|
| **Coprecipitates from Mixed Arsenate/Sulfate Solutions** | | | | | | | | |
| 0 | 480 | 0 | 41 | 0.00 | 0.15 | 0.000 | 184 | 8.9 YR 6.5/8.8 |
| 0.02 | 465 | 22 | 31 | 0.04 | 0.12 | 0.233 | 54 | 8.7 YR 6.6/8.8 |
| 0.041 | 454 | 44 | 27 | 0.07 | 0.10 | 0.411 | 84 | 8.2 YR 6.5/8.1 |
| 0.085 | 395 | 77 | 21 | 0.14 | 0.09 | 0.611 | 88 | 7.7 YR 6.5/7.9 |
| 0.178 | 408 | 147 | 17 | 0.27 | 0.07 | 0.787 | 80 | 8.1 YR 6.8/7.1 |
| 0.394 | 360 | 202 | 15 | 0.42 | 0.07 | 0.852 | 105 | 8.2 YR 6.9/6.2 |
| 0.661 | 335 | 237 | 10 | 0.53 | 0.05 | 0.910 | 104 | 7.6 YR 6.3/6.3 |
| 1.0 | 310 | 250 | 0 | 0.60 | 0.00 | 1.0 | 126 | 7.8 YR 6.3/6.0 |
| **"Amorphous" Iron$^{III}$ Arsenate (*13*)** | | | | | | | | |
| 1.0 | 286 | 405 | 0 | 1.06 | 0.00 | 1.0 | 130 | 1.6 Y 8.2/4.0 |
| **Sorption Samples** | | | | | | | | |
| Sh+As[c] | 423 | 175 | 18 | 0.31 | 0.07 | 0.806 | 180 | 8.9 YR 6.5/8.8 |
| Fh+As[d] | 410 | 210 | 0 | 0.38 | 0.00 | 1.0 | 226 | 4.2 YR 3.5/4.5 |

[a] SSA, specific surface area. [b] Color according to the Munsell system. Diffuse reflectivity in the visible (0.4−0.8 $\mu$m) range determines the hue (e.g., 4.2 YR), value (e.g., 3.5), and chroma (e.g., 4.5) of the Munsell notation (e.g., 4.2 YR 3.5/4.5). [c] Prepared by sorption of 0.01 M arsenate on pre-prepared schwertmannite at pH 3.0 (24 h equilibration). [d] Prepared by sorption of 0.01 M arsenate on pre-prepared ferrihydrite (2-line) at pH 3.0 (24 h equilibration).

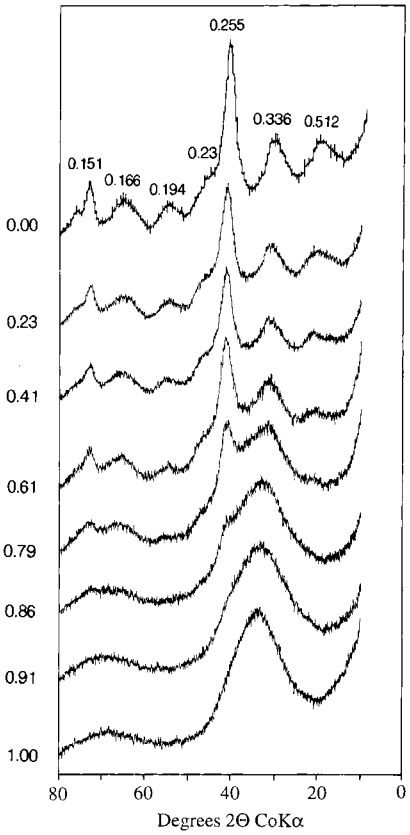


**FIGURE 6. X-ray diffractograms from the synthetic coprecipitates identified by As/(As+S) mole ratios of the solids. Peak positions are in nm.**

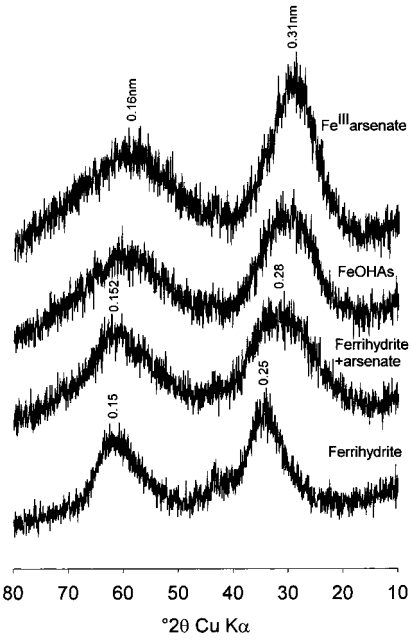


**FIGURE 7. X-ray diffractograms from "amorphous" iron$^{III}$ arsenate prepared according to Krause and Ettel (*13*), FeOHAs, and 2-line ferrihydrite before and after sorption of arsenate (60 d equilibration). Peak positions are in nm.**

>100 $m^2$/g, the acicular aggregates are lost, and the particles become granular (Figure 3d) with individual diameters of 10 nm or less. Thus, the morphology of the FeOHAs particles is clearly different from that of schwertmannite.

**FTIR Data.** Infrared spectra from most of the coprecipitates include absorption bands due to $\nu_1$ ($SO_4$) at 970 $cm^{-1}$, $\nu_4$ ($SO_4$) at 610 $cm^{-1}$, and a splitting of the $\nu_3$ fundamental of $SO_4$ to yield features at 1210, 1130, and 1040 $cm^{-1}$ (Figure 9). These bands, along with those at 700 and 3370 $cm^{-1}$ (OH stretching vibration), are typical of schwertmannite (*18*).

The frequency of the OH stretching vibration at 3370 $cm^{-1}$ shifts to approximately 3010 $cm^{-1}$ with increasing As content (Figure 9a) and is consistent with the results of Myneni et al. (*26*) for solvated arsenate. All sulfate bands diminish with increasing As/(As+S) and are gradually replaced by a broad, asymmetric absorption feature centered at 840 $cm^{-1}$ (Figure 9b). A similar band has been assigned to As−O stretching in studies of crystalline scorodite (*26*), amorphous iron$^{III}$ arsenate (*28*), and arsenate sorbed on iron$^{III}$ oxides (*25*, *29*). The 700-$cm^{-1}$ band attributed to OH stretching in schwertmannite is lost when As/(As+S) exceeds 0.8 leaving a residual absorption feature at 657 $cm^{-1}$ (Figure 9c) that is currently unassigned. The intensity of the 700 $cm^{-1}$ schwertmannite band is also negatively correlated with the 840 $cm^{-1}$ arsenate band and confirms that the schwertmannite structure is disrupted by the incorporation of coprecipitated As.

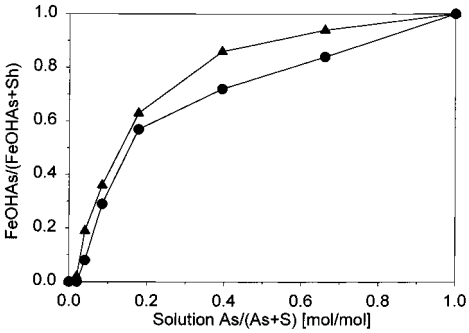


**FIGURE 8. Relationship between the initial As/(As+S) mole ratio in solution and the proportion of iron$^{III}$ hydroxyarsenate (FeOHAs) and schwertmannite (Sh) formed as estimated by XRD (▲) and Mössbauer spectroscopy (●).**

**TABLE 4. Mössbauer Data for Synthetic Coprecipitates at Room Temperature (RT) and 4.2 K**

| solid | 298 K (RT) | | | | | 4.2 K | |
|---|---|---|---|---|---|---|---|
| As/(As+S) (mol/mol) | $IS_1$ (mm/s) | $QS_1$ (mm/s) | $IS_2$ (mm/s) | $QS_2$ (mm/s) | $B_{hf}$ (T) | $IS_{av}$[a] (mm/s) | RA[b] (%) |
| 0 | 0.253 | 0.57 | 0.257 | 0.87 | 46.1 | 0.244 | 0 |
| 0.233 | 0.259 | 0.60 | 0.262 | 0.87 | 46.3 | 0.252 | 0 |
| 0.411 | 0.259 | 0.62 | 0.257 | 0.91 | 45.7 | 0.266 | 7 |
| 0.611 | 0.262 | 0.62 | 0.261 | 0.93 | 45.1 | 0.294 | 23 |
| 0.787 | 0.263 | 0.63 | 0.265 | 1.00 | 44.8 | 0.312 | 50 |
| 0.852 | 0.272 | 0.65 | 0.266 | 1.06 | 43.9 | 0.302 | 66 |
| 0.910 | 0.274 | 0.61 | 0.266 | 1.05 | 43.2 | 0.311 | 81 |
| 1.0 | 0.278 | 0.60 | 0.268 | 1.03 | 41.9 | 0.357 | 100 |

[a] $IS_{av}$, the average isomer shift at RT and 4.2 K. [b] Relative area of the FeOHAs component from a simultaneous fit of the RT and 4.2 K spectra.

**Mössbauer Data.** Mössbauer spectra of products from the synthetic coprecipitates at RT consist of doublets indicating (super-) paramagnetic character (spectra not shown). Best fits of the spectra require using the sum of two Lorentzian doublets and are consistent with the presence of two phases (Table 4). The quadrupole splitting of the outer doublet ($QS_2$) increases with increasing As/(As+S) up to 0.852 mol/mol, above which it levels off. The highest QS values for this doublet are much greater than those of schwertmannite ($QS_1$) or even the most poorly crystalline ferrihydrite (*30*) and document distortion of Fe(O,OH) octahedra due to the interaction with arsenate. For the inner doublet, there is an increase in the isomer shift ($IS_1$) that occurs in the same direction as the shift associated with the weak asymmetry in the RT spectrum of schwertmannite (*18*).

Mössbauer spectra from the synthetic coprecipitates at 4.2 K consist of broadened, asymmetric sextets (Figure 5c,d). The magnetic hyperfine field ($B_{hf}$) of the FeOHAs phase with the highest As/(As+S) mole ratio is 41.9 T at 4.2 K (Table 4) and is much lower than that of either schwertmannite (46.1 T) or 2-line ferrihydrite (ca 49.3 T) (*30*). This effect can be attributed to magnetic dilution from diamagnetic As throughout the sample resulting in reduced superexchange interactions between neighboring Fe ions and indicating strong interaction between Fe and arsenate. The $B_{hf}$ values (Table 4) show no tendency to saturate with increasing As and suggest that the structure of FeOHAs can tolerate even more arsenate. These observations are supported by analysis of the iron$^{III}$ arsenate (As/Fe = 1) prepared by the method of Krause and Ettel (*13*), which yields a $B_{hf}$ of only 24.8 T and a sextet that is strongly broadened and partially collapsed even at 4.2 K (Figure 4e). At 2.5 and 1.5 K, the hyperfine field of this sample reaches values of 41.5 and 42.3 T, respectively, which are close to that of the coprecipitate with As/(As + S) = 1. These data indicate that the value at 1.5 K is near the saturation hyperfine field, despite strong broadening.

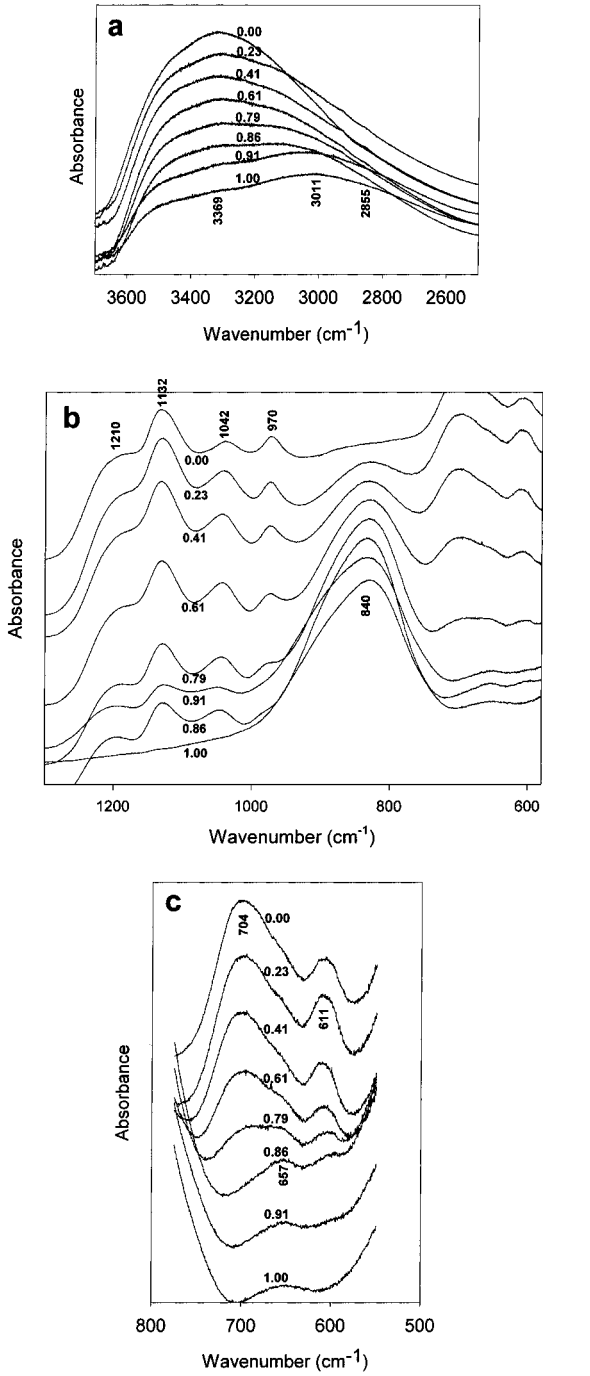


**FIGURE 9. DRIFT spectra from the synthetic coprecipitates identified by As/(As+S) mole ratios of the solids (a) 2500−3700, (b) 600−1300, and (c) 550−750 cm$^{-1}$.**

A simultaneous fit of the 4.2 K and RT spectra from each of the coprecipitates was performed assuming the same hyperfine field (at 4.2 K) and quadrupole splitting (at RT) for the schwertmannite component in each spectrum and likewise for the FeOHAs component. The relative areas of schwertmannite and FeOHAs were assumed to be the same at 4.2 K and RT but different for the individual precipitates. This procedure yielded hyperfine fields of $B_{hf}$ = 46.1 T for schwertmannite and 41.6 T for FeOHAs along with quadrupole splittings of QS = 0.49 mm/s for schwertmannite and QS = 1.03 mm/s for FeOHAs. The relative areas of the FeOHAs component thus calculated (Table 4) are in good agreement with those obtained by XRD analysis (Figure 8).

**Sorption Samples.** The equilibration of pre-prepared schwertmannite and 2-line ferrihydrite with 0.01 M arsenate solutions at pH 3.0 gave products with higher As contents (Table 3) than any of the natural samples (Table 2) but within the range achieved for schwertmannite by coprecipitation from mixed arsenate/sulfate solutions. Sorption did not alter the color of the samples as observed by Rancourt et al. (*10*) for natural, arsenic ferrihydrites but did have an effect on other properties. For example, As sorption on schwertmannite effectively displaced ca. 60% of the sulfate from the original sample (Table 3), and the sensitive (200,111) XRD peak diminished in intensity after only 24 h contact (not shown). No further mineralogical alterations were noted after 60 d contact. Arsenate sorption was even greater on the 2-line ferrihydrite because of its larger surface area (Table 3). Sorption also caused the XRD peaks of ferrihydrite to broaden and shift toward those of FeOHAs and amorphous iron$^{III}$ arsenate (Figure 7). Similar peak shifts were observed by Rancourt et al. (*10*) for natural, arsenic ferrihydrites formed by coprecipitation.

Our laboratory studies demonstrate the aggressive character of the arsenate ion at low pH and also indicate that similar products can be obtained at As/Fe mole ratios <0.15 irrespective of whether the dominant process is coprecipitation or sorption of arsenate on existing schwertmannite or ferrihydrite. No direct evidence was obtained for the presence of FeOHAs in the natural samples. However, it seems reasonable that FeOHAs could develop either as a coprecipitate or as a surface phase on schwertmannite/ferrihydrite formed in natural systems or process waste streams containing relatively low concentrations of dissolved arsenate. At the low pH (2−4) associated with most acid mine drainage, schwertmannite is probably an important host mineral for arsenate, and its sorption properties should be examined in greater detail.

## Acknowledgments

The authors gratefully recognize Dr. Maunu Härme for originally suggesting the Paroistenjärvi Mine as a study site. Dr. Antti Vuorinen and Mrs. Marja Pitkänen performed most of the chemical analyses. Dr. S. Myneni assisted with the FTIR results. Ms. Satu Moberg and Mr. F. S. Jones assisted with the preparation of graphics. Financial support was provided to L.C. by the Maj and Tor Nessling Foundation, to J.M.B. by the Alexander von Humboldt Stiftung and the Deutscher Akademischer Austauschdienst, and to U.S. and F.W. by the Deutsche Forschungsgemeinschaft (Schw. 90-51).

## Literature Cited

(1) Morton, W. E.; Dunnette, D. A. In *Arsenic in the Environment, Part 2: Human Health and Ecosystem Effects*; Nriagu, J. O., Ed; Wiley: New York, 1994; pp 17−34.

(2) Gonzalez, V. L. E.; Monhemius, A. J. In *Arsenic Metallurgy Fundamentals and Applications*; Reddy, R. G., Hendrix, J. L., Queneau, P. B., Eds; Symposium Procedings of TMS-AIME Annual Meeting, Phoenix, AZ, 1988; TMS-AIME: 1988; pp 405−453.

(3) Carlson, L.; Lindström, E. B.; Hallberg, K. B.; Tuovinen, O. H. *Appl. Environ. Microbiol.* **1992**, *58*, 1046−1049.

(4) Tuovinen O. H.; Bhatti, T.M.; Bigham, J. M.; Hallberg, K. B.; Garcia, Jr., O.; Lindström, E. B. *Appl. Environ. Microbiol.* **1994**, *60*, 3268−3274.

(5) Bowell R. J.; Morley, N. H.; Din, V. K. *Appl. Geochem*. **1994**, *9*, 15−22.

(6) Leblanc, M.; Archard, B.; Othman, D. B.; Luck, J. M.; Bertrand-Sarfatti, J.; Personné, J. Ch. *Appl. Geochem*. **1996**, *11*, 541−554.

(7) Raven, K. P.; Jain, A.; Loeppert, R. H. *Environ. Sci. Technol*. **1998**, *32*, 344−349.

(8) Dunn P. J. *Mineral. Mag.* **1982**, *46*, 261−264.

(9) Pichler, T.; Veizer, J.; Hall, G. E. M. *Environ. Sci. Technol*. **1999**, *33*, 1373−1378.

(10) Rancourt, D. G.; Fortin, F.; Pichler, T.; Thibault, P.-J.; Lamarche, G.; Morris, R. V.; Mercier, P. H. J. *Am. Mineral*. **2001**, *86*, 834−851.

(11) Dove, P. M.; Rimstidt, J. D. *Am. Mineral.* **1985**, *70*, 838−844.

(12) Robins, R. G. *Am. Mineral.* **1987**, *72*, 842−844.

(13) Krause, E.; Ettel, V. A. *Am. Mineral.* **1988**, *73*, 850−854.

(14) Papassiopi, N.; Stefanakis, M.; Kontopoulus, A. In *Arsenic Metallurgy Fundamentals and Applications*; Reddy, R. G., Hendrix, J. L., Queneau, P. B., Eds.; Symposium Proceedings of TMS-AIME Annual Meeting, Phoenix, AZ, 1988; TMS-AIME: 1988; pp 321−334.

(15) Krause, E.; Ettel, V. A. *Hydrometallurgy* **1989**, *22*, 311−337.

(16) Robins, R. G.; Huang, J. C. Y.; Nishimura, T.; Khoe, G. H. In *Arsenic Metallurgy Fundamentals and Applications*; Reddy, R. G., Hendrix, J. L., Queneau, P. B., Eds,; Symposium Proceedings of TMS-AIME Annual Meeting, Phoenix, AZ, 1988; TMS-AIME: 1988; pp 99−112.

(17) Waychunas, G. A.; Rea, B. A.; Fuller, C. C.; Davis, J. A. *Geochim. Cosmochim. Acta* **1993**, *57*, 2251−2269.

(18) Bigham, J. M.; Schwertmann, U.; Carlson, L.; Murad, E. *Geochim. Cosmochim. Acta* **1990**, *54*, 2743−2758.

(19) Bigham, J. M.; Schwertmann, U.; Carlson L. In *Biomineralization Processes of Iron and Manganese: Modern and Ancient Environments*; Skinner, H. C. W., Fitzpatrick, R. W., Eds.; Catena Suppl. 21, Catena Verlag: Cremlingen-Destedt, 1992; pp 219−232.

(20) Bigham, J. M.; Carlson, L.; Murad, E. *Mineral. Mag.* **1994**, *58*, 641−648.

(21) Marshall, N. J. *J. Geochem. Explor.* **1978**, *10*, 307−313.

(22) De Endredy, A. S. *Clay Miner. Bull.* **1963**, *5*, 209−217.

(23) Janik, L. M.; Raupach, M. *CSIRO Div. Soils Tech. Pap*. **1977**, *No. 35*, 1−37.

(24) Friedl, J.; Schwertmann, U. *Clay Miner.* **1996**, *31*, 455−464.

(25) Lumsdon, D. G.; Fraser, A. R.; Russel, J. D.; Livesey, N. T. *J. Soil Sci.* **1984**, *35*, 381−386.

(26) Myneni, S. C. B.; Traina, S. J.; Waychunas, G. A.; Logan, T. J. *Geochim. Cosmochim. Acta* **1998**, *62*, 3285−3300.

(27) Winland, R. L.; Traina, S. J.; Bigham, J. M. *J. Environ. Qual.* **1991**, *20*, 452−460.

(28) Makhmetov, M. Z.; Sagadieva, A. K.; Chuprakov, V. I. *J. Appl. Chem. (USSR)* **1981**, *54*, 823−824.

(29) Harrison, J. B.; Berkheiser, V. E. *Clays Clay Miner.* **1982**, *30*, 97−102.

(30) Murad, E.; Schwertmann, U. *Am. Mineral.* **1980**, *65*, 1044−1049.

*Received for review June 4, 2001. Revised manuscript received January 15, 2002. Accepted January 23, 2002.*

ES0110271